EARTHQUAKE ENGINEERING AND STRUCTURAL DYNAMICS, VOL. 23, 1165–1180 (1994)

WAVE DISPERSION AND OPTIMAL MASS MODELLING FOR ONE-DIMENSIONAL PERIODIC STRUCTURES

NOBUO FUKUWA* AND SHINICHI MATSUSHIMA

Department of Architecture, School of Engineering, Nagoya University, Furo-cho, Chikusa-ku, Nagoya 464-01, Japan

SUMMARY

Discrete analysis methods are frequently used for the study of the structure and soil. However, the assumption of the displacement interpolation function makes the waves dispersive, which means the numerical dispersion. The wave dispersion induced by the discretization depends on the mass modelling. Also, the existence of added lumped masses makes waves dispersive even for the continuum modelling. In order to examine these wave dispersions, a one-dimensional periodic structure is adopted as an analysis model and the dynamic transfer matrix method is applied. A wave solution and a finite element solution are used for the evaluation of the transfer matrix. The phase and group velocities in the structure are explicitly represented. These values are compared among the continuum modelling and the discretization modelling in which several consistent mass ratios are adopted. The optimal consistent mass ratio, which makes the wave velocity of the discrete model the same as that of the continuum model, is newly developed here. The validity of this mass modelling technique is presented by examining the frequency response function and impulse response function.

1. INTRODUCTION

Beam-like structures consist of a sequence of identical segments which are connected to each other. Such structures, which are called periodic structures, are frequently found both in high-rise buildings on earth and Large Space Structures (LSSs) in space. Then, the dynamic properties of periodic structures are a fundamental research theme in structural dynamics.

On earth, disturbances due to traffic loads such as trains and automobiles become important in the design of facilities enclosing precision machines or buildings near stations. In space, the impact loads such as artificial debris are critical ones in the design of LSSs. Since these forces may have a wide band of frequencies, it is necessary to study wave propagation in periodic, beam-like structures at high frequencies.

This paper examines the effect of periodically spaced masses on propagating waves, the validity of the finite elements for the analysis in high frequency range, and the new approach of mass modelling. A simple mathematical model of the structure, composed of a continuous rod with periodically spaced lumped masses, is used. This model can represent super-high-rise buildings since the floors behave like lumped masses and the inter-storey aseismic elements behave like shear beams. Also, the beam-like trusses in space structures composed of flexible pipes and rigid joints can be considered by the periodic model. Therefore, this fundamental study of wave propagation in one-dimensional periodic structures may be useful in understanding both the dynamic response of super-high-rise buildings and the dynamic response of LSSs.

Since the work by Brillouin,[1] many studies[2–5] on periodic structures have been presented. This research field has recently been accelerated due to its importance in the analysis of LSSs. Periodic structures have many interesting features. They have pass and stop frequency bands, they act as wave guides that propagate many kinds of waves, and they can be considered as mechanical filters. There are two (analysis) approaches to periodic structures. One approach is based on wave-propagation theory[2,3] and the other is based on transfer matrix methods[4,5]. The latter uses a transfer matrix which is determined from the fundamental repeating element of the structure. The transfer matrix method has been applied to static and dynamic structural

* Associate Professor.

CCC 0098–8847/94/111165–16

Received 22 October 1993
Revised 18 January 1994

analysis,[6] and wave-propagation analysis in soils.[7] The method seems to be the most powerful for dynamic analysis of periodic structures.

The transfer matrix may be derived from discrete methods, such as the finite element method, to obtain results for complicated geometries and arbitrary boundary conditions quickly. However, the range of analysis of such transfer matrices is limited to a low frequency range. An exact transfer matrix can be obtained by continuum equations within the fundamental structural element. However, for large periodic structures, the method may suffer from numerical instabilities. Recently, Yong and Lin[5] showed that this numerical instability can be eliminated by using the characteristics of the eigenvalues of the transfer matrix.

In this paper, the wave propagation characteristics of a rod with periodically spaced masses is examined over a wide frequency range. The wave solution as well as finite element solution are applied to the transfer matrix method and the basic ideas in Yong and Lin[5] are simplified and adopted. The resulting method is accurate for a periodic structure composed of any number of structure elements. After introducing non-dimensional quantities, explicit expressions are developed for the pass and stop bands, the phase and group velocities, and an attenuation rate. These results give clear physical insight into the wave propagation and dynamic characteristics of the structure.

In order to grasp the effect of the discretization, wave propagation in the discrete model is compared with that of the continuum model. The discrete model consists of massless springs and discrete or consistent masses. By examining the effect of mass modelling, it is clarified that the discrete solution becomes dispersive and this numerical dispersion depends on the mass modelling. Then, by matching the discrete and continuous results, an optimal discrete model is developed. This optimal mass model drastically improves the discrete solution. Many mass modelling techniques[8–10] have been proposed up to now while the study on wave propagation seems not to have been examined in detail.

2. WAVE PROPAGATION OF CONTINUUM MODEL

Consider the one-dimensional periodic structure composed of a continuum body (beam or rod) with $n+1$ equally spaced lumped masses, as shown in Figure 1. Denote the mass of each lumped mass by m, the distance between masses by l, and the shear (or Young's) modulus, section area and mass density of the continuum body by G (or E), A and ρ. A source of excitation is given by a prescribed displacement applied to the left boundary (node 0).

The fundamental structural element of this problem is a continuum body of length l attached to lumped masses of mass $m/2$ at both ends, as shown in Figure 1(b). The dynamic stiffness matrix $\mathbf{S}$ of circular frequency ω for shear beam (or axial rod) is obtained by using the wave solution of the one-dimensional continuum:

$$\mathbf{S} = \frac{GA\dfrac{\omega l}{\sqrt{G/\rho}}}{l\sin\dfrac{\omega l}{\sqrt{G/\rho}}}\begin{bmatrix} \cos\dfrac{\omega l}{\sqrt{G/\rho}} & -1 \\ -1 & \cos\dfrac{\omega l}{\sqrt{G/\rho}} \end{bmatrix} - \frac{\omega^2}{2}\begin{bmatrix} m & 0 \\ 0 & m \end{bmatrix} \tag{1}$$

To simplify the above equation, the following quantities are introduced:

$$k_b = \frac{GA}{l}, \qquad \alpha = \frac{m}{\rho A l}, \qquad \beta = \frac{\omega}{V} l, \qquad V = \sqrt{\frac{G}{\rho}} \tag{2}$$

Here, k_b is the static spring constant of the one-dimensional continuum with length l, α is the mass ratio of the lumped mass to the continuum, β is a non-dimensional frequency and V is the body wave velocity. Material damping can be included by using a complex elastic modulus. Applying equation (2) to equation (1) yields a simpler form for the dynamic stiffness matrix:

$$\mathbf{S} = k_b \frac{\beta}{\sin\beta}\begin{bmatrix} -\dfrac{\alpha\beta}{2}\sin\beta + \cos\beta & -1 \\ -1 & -\dfrac{\alpha\beta}{2}\sin\beta + \cos\beta \end{bmatrix} \tag{3}$$

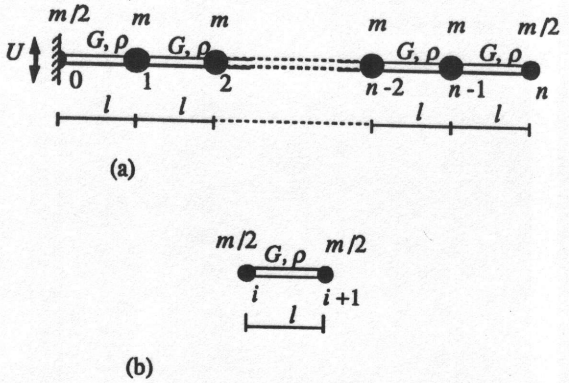

Figure 1. Analytical models: (a) one-dimensional periodic structure; (b) fundamental structural element

The transfer matrix **T** is derived directly from **S** as follows:

$$\mathbf{T} = \begin{bmatrix} -\mathbf{S}_{12}^{-1}\mathbf{S}_{11} & \mathbf{S}_{12}^{-1} \\ -\mathbf{S}_{21} + \mathbf{S}_{22}\mathbf{S}_{12}^{-1}\mathbf{S}_{11} & -\mathbf{S}_{22}\mathbf{S}_{12}^{-1} \end{bmatrix}$$

$$= \begin{bmatrix} -\dfrac{\alpha\beta}{2}\sin\beta + \cos\beta & -\dfrac{1}{k_b}\dfrac{\sin\beta}{\beta} \\ k_b\dfrac{\beta}{\sin\beta}\left\{1 - \left(-\dfrac{\alpha\beta}{2}\sin\beta + \cos\beta\right)^2\right\} & -\dfrac{\alpha\beta}{2}\sin\beta + \cos\beta \end{bmatrix} \tag{4}$$

The transfer matrix gives the relationship between the state vectors of node i and node $i+1$:

$$\begin{bmatrix} u_{i+1} \\ f_{i+1} \end{bmatrix} = \mathbf{T}\begin{bmatrix} u_i \\ f_i \end{bmatrix} \tag{5}$$

Here, u_i and f_i represent the displacement and force at node i. The eigenproblem of the transfer matrix is

$$\mathbf{T}\Phi = \Phi\Lambda \tag{6}$$

where the eigenvalues Λ and eigenvectors Φ are expressed as follows:

$$\Lambda = \begin{bmatrix} \lambda_1 & 0 \\ 0 & \lambda_2 \end{bmatrix}, \qquad \Phi = [\Phi_1 \quad \Phi_2]$$

By using equations (4)–(6), the eigenvalues and eigenvectors can be solved, yielding

$$\lambda_i = \left(-\frac{\alpha\beta}{2}\sin\beta + \cos\beta\right) \pm \sqrt{\left(-\frac{\alpha\beta}{2}\sin\beta + \cos\beta\right)^2 - 1}$$

$$\Phi = \begin{bmatrix} -1 \\ \pm k_b\dfrac{\beta}{\sin\beta}\sqrt{\left(-\dfrac{\alpha\beta}{2}\sin\beta + \cos\beta\right)^2 - 1} \end{bmatrix} \tag{7}$$

An important feature of the eigenvalues of the transfer matrix is that they are reciprocals of each other,[4] i.e., $\lambda_1\lambda_2 = 1$. For the case of no material damping, the eigenvalues are real valued when the expression in the

radical in equation (7) is positive, and the eigenvalues form a complex conjugate pair when this expression is negative. For consistency, we assign mode numbers such that $|\lambda_1| \leqslant 1$. Then, λ_1 corresponds to a propagating wave and λ_2 corresponds to a reflecting wave. To make sure the mode numbers are consistent, the sign of the radicals in equation (7) should be positive when $2j\pi \leqslant \beta < (2j+1)\pi$ and negative when $(2j+1)\pi \leqslant \beta < 2(j+1)\pi$. Since the eigenvalues are reciprocals, we can denote $\lambda_1 = \lambda$ and $\lambda_2 = 1/\lambda$. Then, λ is given by

$$\lambda = \left(-\frac{\alpha\beta}{2}\sin\beta + \cos\beta\right) + \sqrt{\left(-\frac{\alpha\beta}{2}\sin\beta + \cos\beta\right)^2 - 1} \qquad \text{for } 2j\pi \leqslant \beta < (2j+1)\pi$$

$$= \left(-\frac{\alpha\beta}{2}\sin\beta + \cos\beta\right) - \sqrt{\left(-\frac{\alpha\beta}{2}\sin\beta + \cos\beta\right)^2 - 1} \qquad \text{for } (2j+1)\pi \leqslant \beta < 2(j+1)\pi \tag{8}$$

From equation (6), the nth power of the transfer matrix is given by

$$\mathbf{T}^n = \Phi\Lambda^n\Phi^{-1} \tag{9}$$

Combining equations (5) and (9) yields the global equation of the periodic structure

$$\begin{bmatrix} u_n \\ f_n \end{bmatrix} = \Phi\Lambda^n\Phi^{-1}\begin{bmatrix} u_0 \\ f_0 \end{bmatrix} \tag{10}$$

One important property of equation (10) is that when $\lambda_2 = 1/\lambda > 1$, the matrix Λ^n may suffer numerical instability when n becomes large. To avoid this instability, we introduce generalized state vectors[5] as

$$\begin{bmatrix} u_i \\ f_i \end{bmatrix} = \Phi\begin{bmatrix} \xi_i \\ \eta_i \end{bmatrix} \tag{11}$$

Substituting this relationship into equation (10) yields

$$\begin{bmatrix} \xi_n \\ \eta_n \end{bmatrix} = \begin{bmatrix} \lambda^n & 0 \\ 0 & \lambda^{-n} \end{bmatrix}\begin{bmatrix} \xi_0 \\ \eta_0 \end{bmatrix} = \begin{bmatrix} \lambda^n\xi_0 \\ \lambda^{-n}\eta_0 \end{bmatrix} \tag{12}$$

Denote the wave vector at the left boundary by

$$\begin{bmatrix} \xi_0 \\ \eta_0 \end{bmatrix} = \begin{bmatrix} \xi \\ \eta \end{bmatrix}$$

Then, equation (12) yields four equations from the boundary conditions. When a displacement U is prescribed at node 0, and node n is free, the equations are

$$\begin{aligned} \Phi_{11}\xi + \Phi_{12}\eta &= U \\ \Phi_{11}\lambda^n\xi + \Phi_{12}\lambda^{-n}\eta &= u_n \\ \Phi_{21}\xi + \Phi_{22}\eta &= f_0 \\ \Phi_{21}\lambda^n\xi + \Phi_{22}\lambda^{-n}\eta &= 0 \end{aligned} \tag{13}$$

Equations (11) and (13) can be solved to obtain the state values at nodes 0 and n. The results are

$$f_0 = \frac{\Phi_{21}\Phi_{22}(1-\lambda^{2n})}{\Phi_{11}\Phi_{22}-\Phi_{12}\Phi_{21}\lambda^{2n}}U, \qquad u_n = \frac{\Phi_{11}\Phi_{22}-\Phi_{12}\Phi_{21}}{\Phi_{11}\Phi_{22}-\Phi_{12}\Phi_{21}\lambda^{2n}}\lambda^n U \tag{14}$$

These expressions avoid numerical instability, since they do not contain the potentially large term λ^{-n}.

Equations (10) and (12) show that the eigenvalues of the transfer matrix correspond to the amplification and phase factors of the propagating waves in the fundamental element of the periodic structure. If there is no material damping, the eigenvalues given by equation (8) are either both real or complex valued, as explained earlier. When the eigenvalues are complex, their absolute values are both unity and the wave propagates with a phase delay without decay. On the other hand, if the eigenvalues are real, the wave corresponding to $\lambda = \lambda_1 < 1$ attenuates.

The condition for which the eigenvalues are complex is examined next. Consider the expression in the radical in equation (7). The eigenvalues are complex when this expression is negative. This is equivalent to the following inequality condition:

$$g(\beta) = \left| -\frac{\alpha\beta}{2}\sin\beta + \cos\beta \right| - 1 < 0 \tag{15}$$

Let β_1 and β_2 denote the non-dimensional frequencies which satisfy $g(\beta) = 0$. The definition of $g(\beta)$ in equation (15) yields the following closed-form expressions for these frequencies:

$$\sin\beta_1 = 0, \qquad \tan\beta_2 = \frac{4\alpha\beta_2}{\alpha^2\beta_2^2 - 4} \tag{16}$$

There exist an infinite number of solutions to equation (16), and β_1 and β_2 satisfy

$$\beta_1 = j\pi < \beta_2 \leqslant (j+1)\pi \quad \text{for } j = 0, 1, 2, \cdots \tag{17}$$

The equality in equation (17) corresponds to the case of a homogeneous continuum without lumped masses.

The eigenvalues are complex when

$$\beta_1 = j\pi < \beta < \beta_2 < (j+1)\pi \quad \text{for } j = 0, 1, 2, \cdots \tag{18}$$

and become real for all other frequencies. This is expressed by

$$\begin{aligned} &\lambda_1 = e^{-i\varphi}, \qquad \lambda_2 = e^{i\varphi} \qquad \text{for } j\pi \leqslant \beta \leqslant \beta_2 < (j+1)\pi \\ &|\lambda_1| = |\lambda| < 1, \qquad |\lambda_2| = 1/|\lambda| > 1 \qquad \text{for } j\pi \leqslant \beta_2 < \beta < (j+1)\pi \end{aligned} \tag{19}$$

The eigenvalue λ_1 is the amplification factor of the wave which propagates from node i to node $i+1$ and λ_2 is the amplification factor of the wave which propagates in the opposite direction. Complex λ indicates waves propagating without decay and real λ indicates exponentially decaying waves. The frequency ranges which correspond to complex λ are called pass bands and all other frequency ranges are called stop bands. Figure 2 shows how the absolute values of the eigenvalues λ_1 and λ_2 vary with respect to the mass ratio, α, and the non-dimensional frequency, β. The pass bands are clearly shown in (upper) Figure 2 by the flat portion of the surface. When α and β become large, the range of the pass band decreases and the peak value of $|\lambda_2|$ increases.

The frequency range of the pass band is examined in more detail. Equation (16) shows that as the product $\alpha\beta$ increases, β_2 asymptotically approaches β_1:

$$\lim_{\alpha\beta\to\infty} \beta_2 = \beta_1 + O\left(\frac{1}{\alpha\beta}\right) \tag{20}$$

For large values of $\alpha\beta$, the pass bands collapse to the lines $\beta = j\pi$. Figure 3 illustrates this behaviour by showing plots of $g(\beta)$ for $\alpha = 0$, 1 and 2. Negative values of $g(\beta)$ indicate pass bands and positive values indicate stop bands. When $\alpha = 0$, all of the frequencies are in the pass band, since $g(\beta) \leqslant 0$. When $\alpha = 1$ and 2, there are five pass bands with widths that decrease as α and β increase.

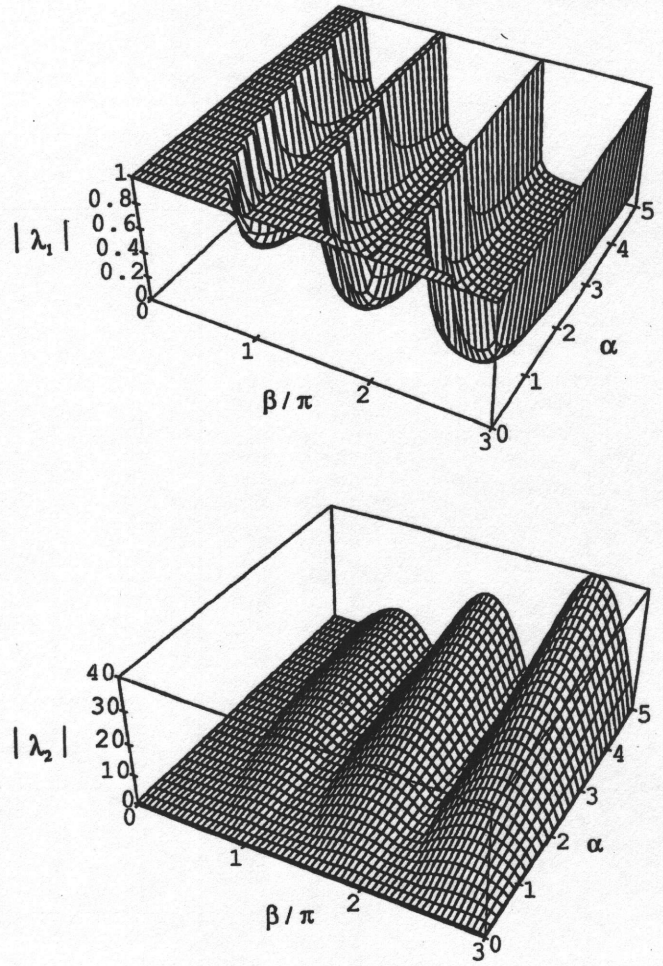

Figure 2. Amplitude of eigenvalue of continuum with added masses

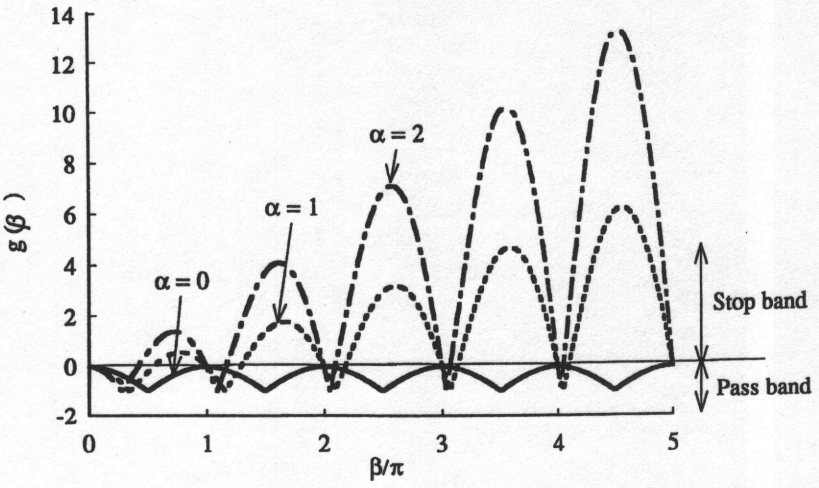

Figure 3. Pass band and stop band

Next, the velocity of the propagating waves is examined. The phase velocity is given in terms of the phase angle of the eigenvalue:

$$V_{\text{phase}} = \frac{\omega l}{\arg(\lambda)} = V\frac{\beta}{\arg(\lambda)} = V\frac{\beta}{\cos^{-1}\left(-\dfrac{\alpha\beta}{2}\sin\beta + \cos\beta\right)} \tag{21}$$

The corresponding group velocity is obtained from the derivative of the phase angle:

$$V_{\text{Group}} = \frac{\partial \omega}{\partial \arg(\lambda)} l = V \frac{\partial \beta}{\partial \arg(\lambda)} = V \left| \frac{\sqrt{4 - (-\alpha\beta \sin\beta + 2\cos\beta)^2}}{(\alpha + 2)\sin\beta + \alpha\beta\cos\beta} \right| \tag{22}$$

These velocities have values only in pass bands, which shows that waves propagate only for frequencies in pass bands and that their phase and group velocities depend on the frequency and the mass ratio.

Finally, the attenuation of waves is examined. To make an analogy with damping vibrations of an oscillator, an attenuation rate is used. Attenuating vibrations decay exponentially with time at a rate $h\omega$, where h is the attenuation rate. In a periodic structure, a wave attenuates or decays as it propagates from one end of a periodic segment to the next by the value $|\lambda|$. The time required for the wave propagation is l/V. Therefore, an attenuation rate h_e is defined by

$$h_e = \frac{1}{\beta} \log|\lambda| = \left| \frac{1}{\beta} \cos^{-1}\left(-\frac{\alpha\beta}{2} \sin\beta + \cos\beta \right) \right| \tag{23}$$

This spatial attenuation rate has a value only in the stop band and this implies that wave attenuation occurs in the stop bands. The attenuation rate depends on the frequency and increases with the mass ratio, α. This is

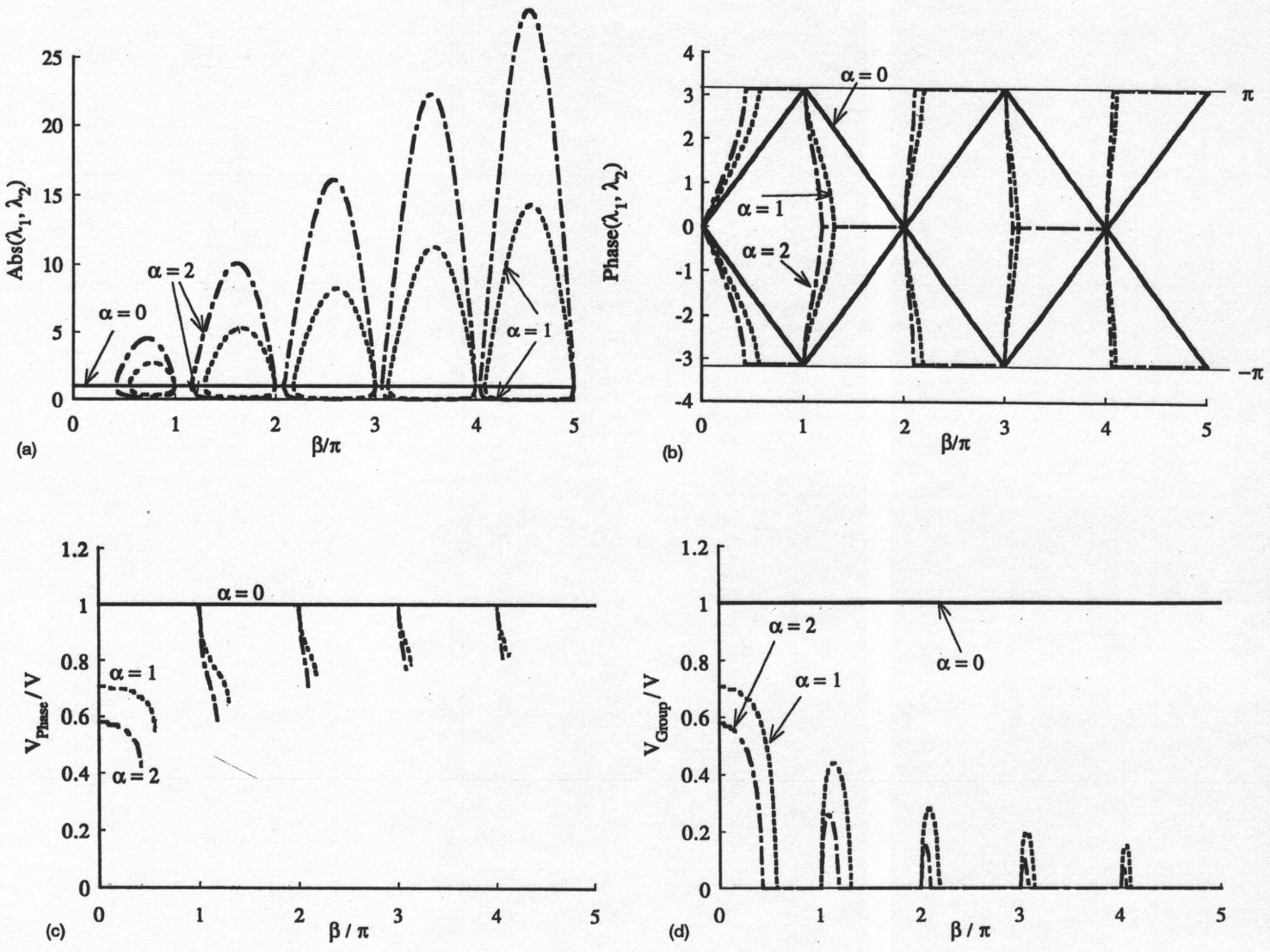

Figure 4. (a)–(d)

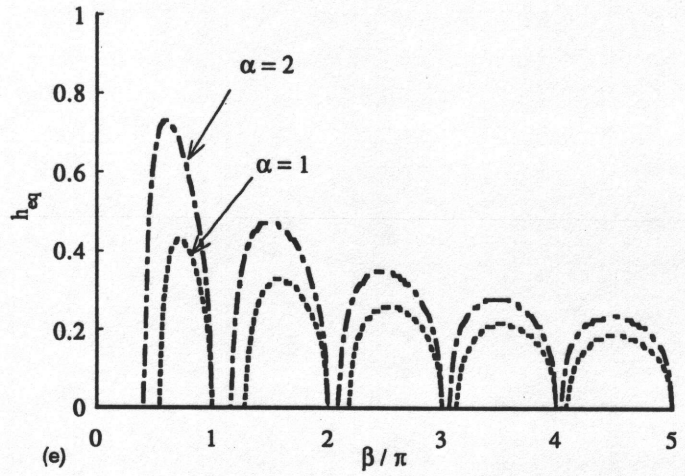

Figure 4. Continuum model: (a) amplitude of eigenvalue; (b) phase angle of eigenvalue; (c) phase velocity; (d) group velocity; (e) attenuation rate

physically explained by the fact that the lumped masses cause reflections which attenuate wave propagation through the structure. When $\alpha = 0$, there are no lumped masses, the attenuation rate is zero, and no wave attenuation occurs. Therefore the existence of the lumped masses produces an attenuating effect.

Figure 4 illustrates the main points of this section. Plots are shown for the absolute value and phase of the eigenvalue, the phase velocity, the group velocity and the attenuation rate. In the pass bands, the phase velocity and group velocity show how the lumped masses cause frequency dependence or dispersion. For non-zero α, the waves propagate with velocities less than that of the body wave in the one-dimensional continuum. The phase velocity is less than the body wave velocity by a factor of $1/\sqrt{1+\alpha}$ at the beginning of the first pass band, and is equal to the body wave velocity at the beginning of all other pass bands. Within each pass band, the phase velocities decrease as the frequency increases and end at the point $(\beta, V_{\text{Phase}}/V) = (\beta_2, \beta_2/(j+1)/\pi)$. The group velocity is equal to the phase velocity at the beginning of the first pass band, and is equal to zero in the beginning of all other pass bands. The group velocity at the end of each pass band is zero. Both the group and phase velocities become slower for increasing mass ratios. In the stop bands, waves do not propagate, and a decaying effect, measured by the attenuation rate, becomes important. The attenuation rate increases with the mass ratio and decreases as the frequency increases.

3. WAVE PROPAGATION OF DISCRETE MODEL

This section analyses a discrete model of the periodic structure and compares the results with those of the continuum model. In the discrete analysis such as the finite element method, a structure is modelled by stiffness and mass matrices. If consistent and discrete mass modellings are combined, the dynamic stiffness matrix of the fundamental structural element becomes

$$\bar{\mathbf{S}} = \frac{GA}{l}\begin{bmatrix} 1 & -1 \\ -1 & 1 \end{bmatrix} - \omega^2\left\{\frac{m}{2}\begin{bmatrix} 1 & 0 \\ 0 & 1 \end{bmatrix} + \rho Al\left(\frac{1-\theta}{2}\begin{bmatrix} 1 & 0 \\ 0 & 1 \end{bmatrix} + \frac{\theta}{6}\begin{bmatrix} 2 & 1 \\ 1 & 2 \end{bmatrix}\right)\right\}$$

$$= k_b\begin{bmatrix} 1 - \dfrac{\beta^2}{2}\left\{(1+\alpha) - \dfrac{\theta}{3}\right\} & -1 - \dfrac{\theta}{6}\beta^2 \\ -1 - \dfrac{\theta}{6}\beta^2 & 1 - \dfrac{\beta^2}{2}\left\{(1+\alpha) - \dfrac{\theta}{3}\right\} \end{bmatrix} \tag{24}$$

Here, θ is the mass ratio of the consistent mass to the total mass of the continuum. For the discrete mass model $\theta = 0$.

The corresponding transfer matrix is obtained as:

$$\bar{\mathbf{T}} = \begin{bmatrix} \dfrac{6-\beta^2\{3(1+\alpha)-\theta\}}{6+\beta^2\theta} & -\dfrac{1}{k_b}\dfrac{6}{6+\beta^2\theta} \\ \dfrac{(1+\alpha)\beta^2 k_b}{6+\beta^2\theta}\left\langle 6-\dfrac{\beta^2}{2}\left\{3(1+\alpha)-2\theta\right\}\right\rangle & \dfrac{6-\beta^2\{3(1+\alpha)-\theta\}}{6+\beta^2\theta} \end{bmatrix} \tag{25}$$

The eigenvalues of this transfer matrix are

$$\bar{\lambda}_i = \frac{6-\beta^2\{3(1+\alpha)-\theta\}}{6+\beta^2\theta} \pm \mathrm{i}\sqrt{1-\left\langle\frac{6-\beta^2\{3(1+\alpha)-\theta\}}{6+\beta^2\theta}\right\rangle^2} \tag{26}$$

Using the definitions in equations (21) and (22), the phase and group velocities are determined from equation (26)

$$\bar{V}_{\text{Phase}} = \frac{\beta V}{\cos^{-1}\left\langle\dfrac{6-\beta^2\{3(1+\alpha)-\theta\}}{6+\beta^2\theta}\right\rangle} \tag{27}$$

$$\bar{V}_{\text{Group}} = \frac{V(6+\beta^2\theta)^2}{36(1+\alpha)\beta}\sqrt{1-\left(\frac{6-\beta^2\{3(1+\alpha)-\theta\}}{6+\beta^2\theta}\right)^2} \tag{28}$$

Equations (27) and (28) show that wave propagates in the frequency range

$$\beta \leqslant 2\sqrt{\frac{3}{3(1+\alpha)-2\theta}} \tag{29}$$

There is only one pass band in the case of the discrete analysis model. Finally, the attenuation rate is given in stop band out of above frequency range:

$$\bar{h}_e = \frac{1}{\beta}\cosh^{-1}\left|\frac{6-\beta^2\{3(1+\alpha)-\theta\}}{6+\beta^2\theta}\right| \tag{30}$$

These results show that the wave velocities of the discrete model vary with β, α and θ, i.e., the frequency, mass ratio of the lumped mass and consistent mass ratio.

Figure 5 shows the phase velocity, group velocity and attenuation rate for a homogeneous continuum ($\alpha = 0$), modelled with various consistent mass ratios. This case corresponds to a problem such as a response of a homogeneous soil subjected to a vertically incident S wave. Unlike the exact continuum model, where the phase and group velocities are always equal to the body wave velocity, the discrete models show numerical dispersion. In the pass frequency band defined by equation (29), the waves propagate with varying velocities, while the attenuating effect emerges in the stop band. As the consistent mass ratio θ increases, the frequency ranges of the pass band become wider, their velocities faster, and the attenuation rate gets smaller. In the lumped mass model ($\theta = 0$), the wave propagates only in the frequency range $\beta \leqslant 2$. In the consistent mass model ($\theta = 1$), waves propagate for a frequency range $\beta \leqslant 2\sqrt{3}$. In these mass modellings, the effect of numerical dispersion cannot be ignored in the frequency range where the value of β is greater than $\pi/6$, which corresponds to a ratio of element length to wave length of 1/12. On the other hand, if the average of the lumped and consistent masses is used ($\theta = 1/2$), the wave velocities are nearly equal to the body wave velocity in the frequency range $\beta \leqslant 1$. Therefore, the consistent mass ratio of $\frac{1}{2}$, which has been recommended by Goudreau[8] and Hughes,[9] seems to be a good choice for discrete models in the case of the homogeneous continuum.

Figure 6 shows the the results for a continuum with added masses ($\alpha = 1$). This case corresponds to problems such as super-high-rise buildings and beam-like trusses in a space structure. Unlike the homogeneous continuum, the consistent mass model shows a good correspondence with the continuum model. However, although pass and stop bands emerge repeatedly in the continuum model, only one pass band exists in the case of the discrete model.

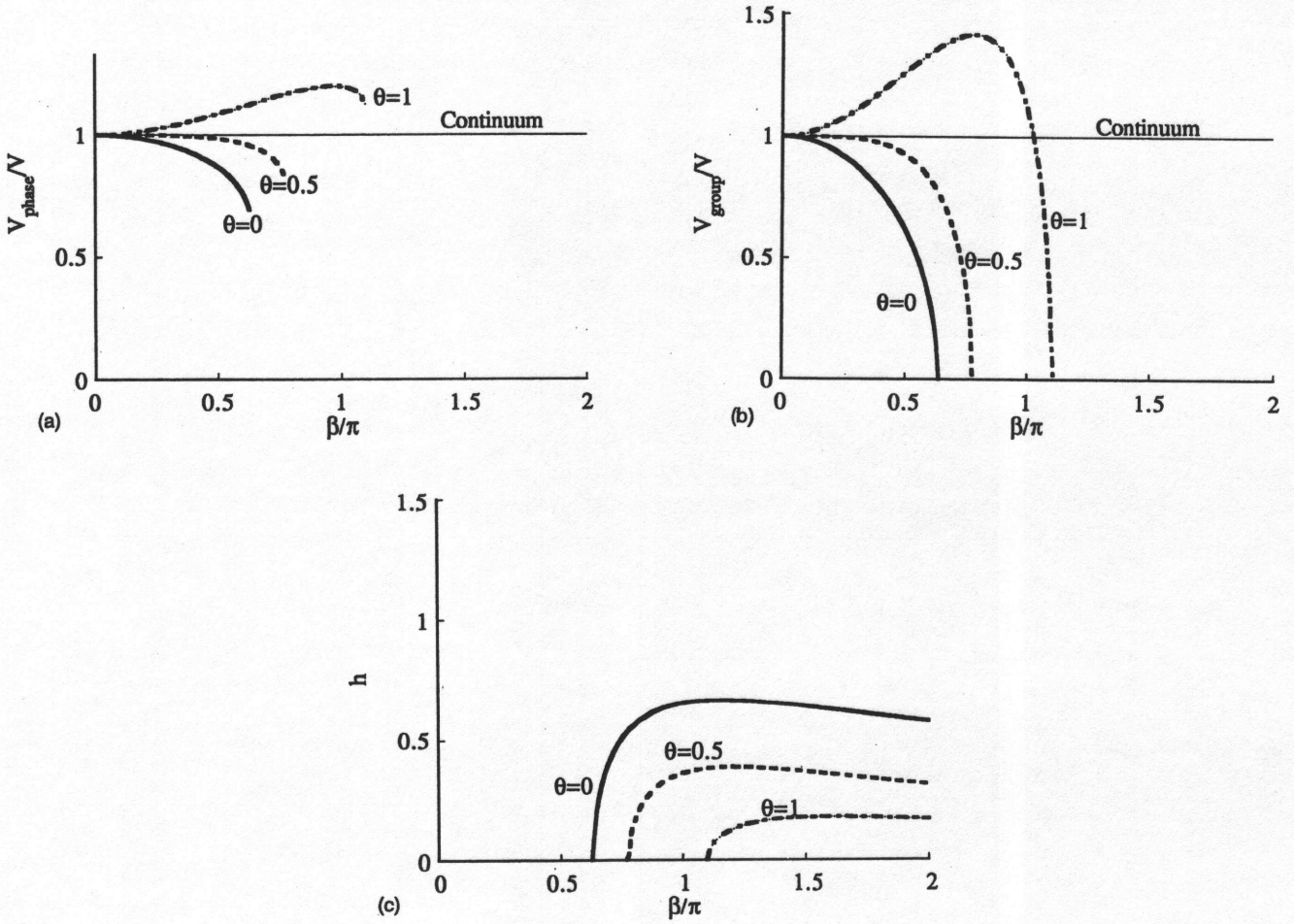

Figure 5. Discrete model ($\alpha = 0{\cdot}0$): (a) phase velocity; (b) group velocity; (c) attenuation rate

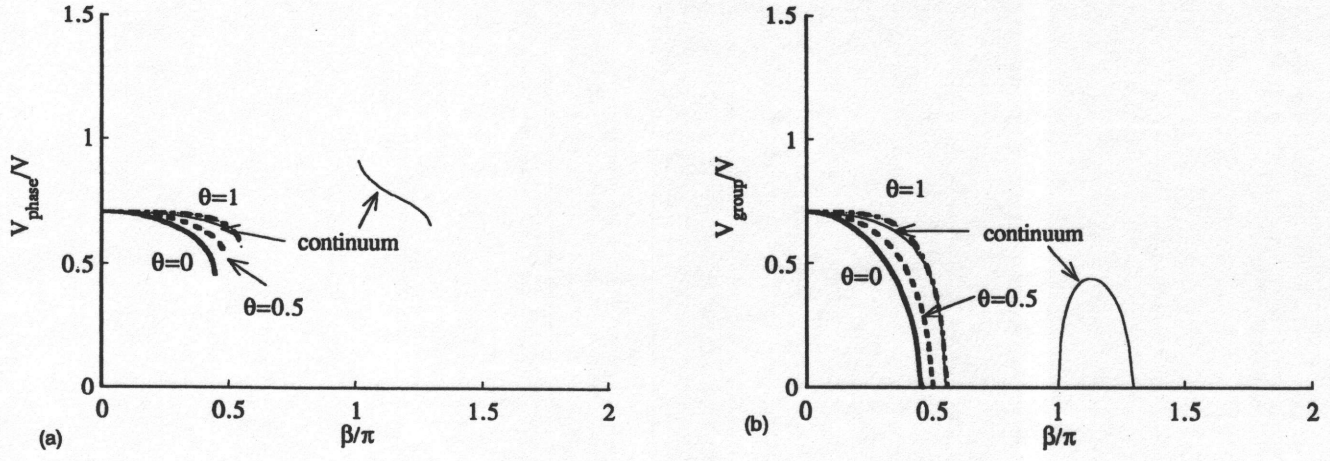

Figure 6. (a)–(b)

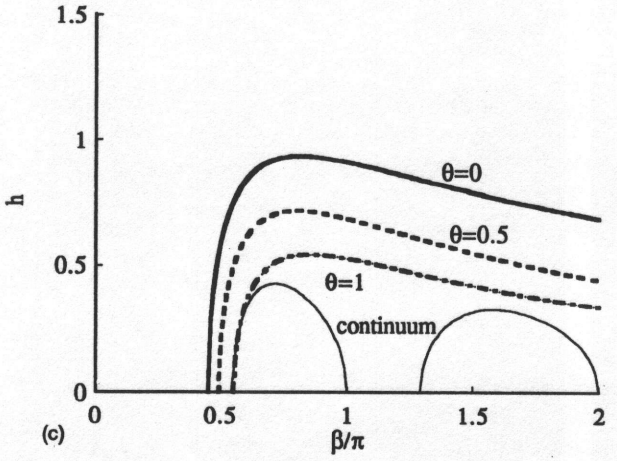

Figure 6. Discrete model ($\alpha = 1{\cdot}0$): (a) phase velocity; (b) group velocity; (c) attenuation rate

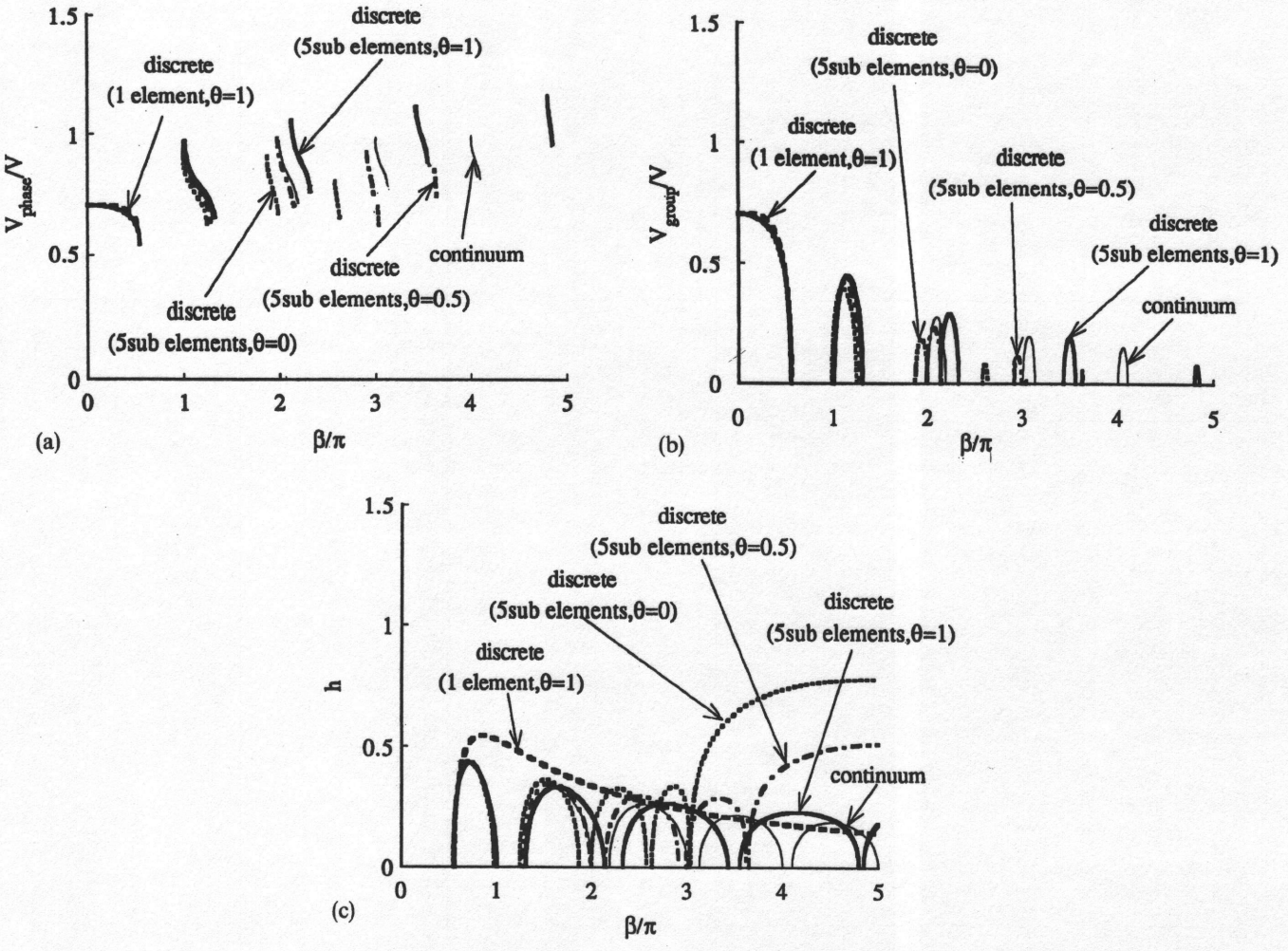

Figure 7. Discrete submeshed model ($\alpha = 1{\cdot}0$): (a) phase velocity; (b) group velocity; (c) attenuation rate

In order to clarify the effect of submeshing, in Figure 7, the corresponding results are presented for a subdivided discrete model. The model used here is a continuum with added masses ($\alpha = 1$), where the continuum is subdivided into five elements. For comparison, the discrete consistent mass model of one element is shown in Figure 7. As shown in this figure, the subdivision makes the pass frequency bands due to the discretization wider, so that the pass and stop bands emerge repeatedly.

4. OPTIMAL MASS MODELLING

In order to improve the accuracy of the discrete model, the consistent mass ratio θ_{opt}, for which the phase velocities, as given by equations (21) and (27), are equal, is evaluated below.

$$\theta_{opt} = 6\,\frac{\beta^2 - 2 + 2\cos\beta - \alpha\beta\sin\beta + \alpha\beta^2}{\beta^2(2 - 2\cos\beta + \alpha\beta\sin\beta)} \tag{31}$$

The same result can be obtained by letting the eigenvalues of the transfer matrix of the discrete model be equal to the ones of the continuum model. When the above consistent mass ratio is used, the pass band is defined by

$$\frac{\alpha\beta}{2}\tan\frac{\beta}{2} = 1 \quad (0 < \beta < \pi) \tag{32}$$

This condition can be derived from the second equation of equation (16). This shows that the dynamic property of the discrete model is fitted to those of the continuum model, in the range of the first pass band. At zero frequency equation (27) becomes

$$\lim_{\beta\to\infty}\theta_{opt} = \frac{2\alpha + 1}{2(\alpha + 1)} \tag{33}$$

In the case of the homogeneous continuum model ($\alpha = 0$), this consistent mass ratio is equal to $\frac{1}{2}$ at zero frequency and increases with frequency, as shown in Figure 8. However, when the lumped masses are added ($\alpha > 0$), the optimal consistent mass ratio becomes large. Also, the optimal consistent mass ratio increases with the non-dimensional frequency β, and the frequency range of the pass band decreases when the lumped mass ratio α increases. This implies that the consistent mass ratio should be selected with respect to the structural property and the frequency.

When using the optimal consistent mass ratio, the dynamic stiffness matrix of equation (24) satisfies the following relationship:

$$\bar{\mathbf{S}}_{opt} = \frac{1 + \alpha}{\frac{2}{\beta}\tan\frac{\beta}{2} + \alpha}\,\mathbf{S} \tag{34}$$

Since the above coefficient becomes less than 1, the discrete model using the optimal mass model leads to a smaller dynamic stiffness compared to that of the continuum model.

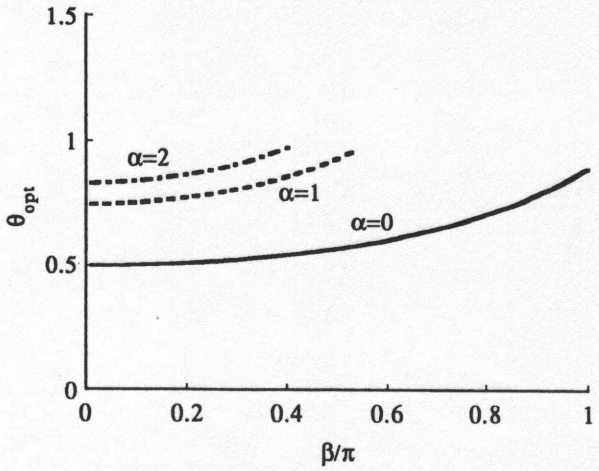

Figure 8. Optimal consistent mass ratio

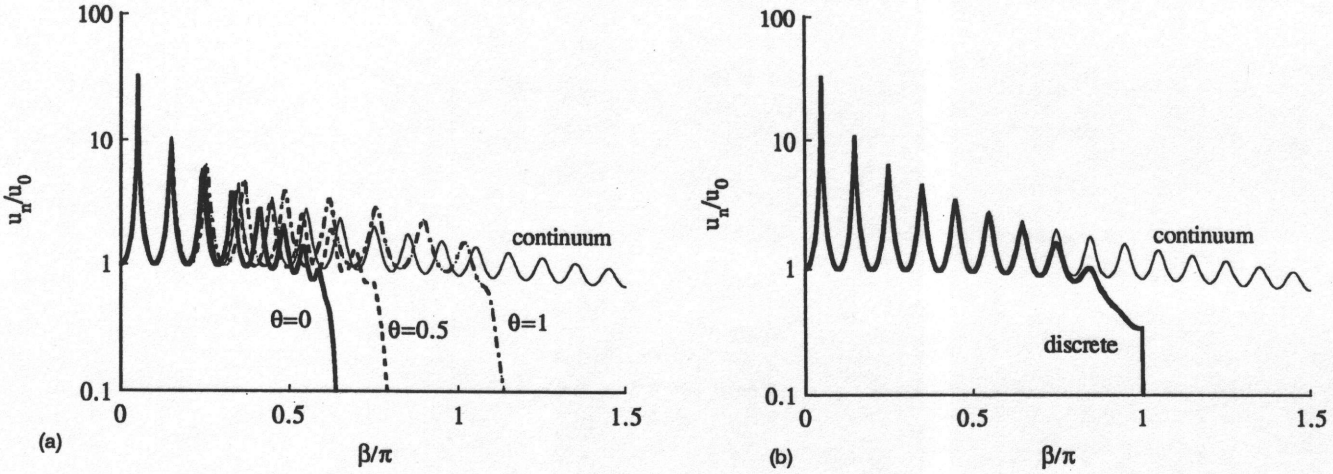

Figure 9. Frequency response function of homogeneous continuum ($\alpha = 0.0$): (a) $\theta = 0, 0.5, 1$; (b) $\theta = \theta_{opt}$

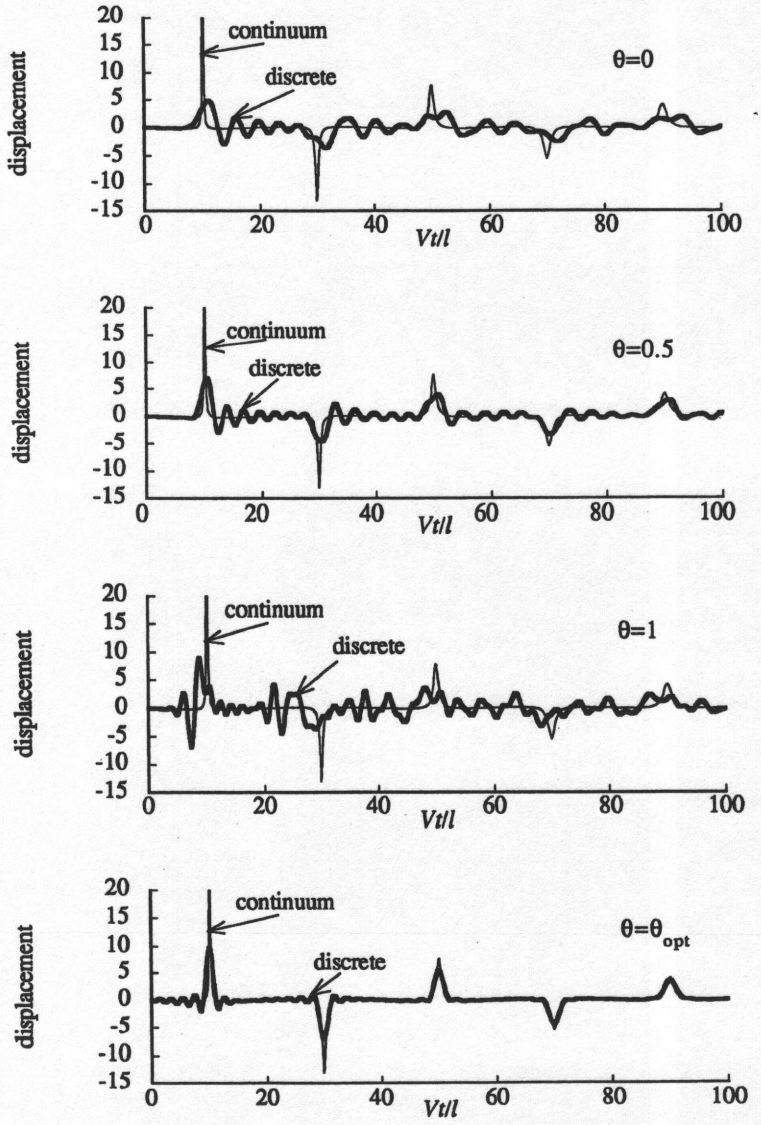

Figure 10. Impulse response function of homogeneous continuum ($\alpha = 0{\cdot}0$)

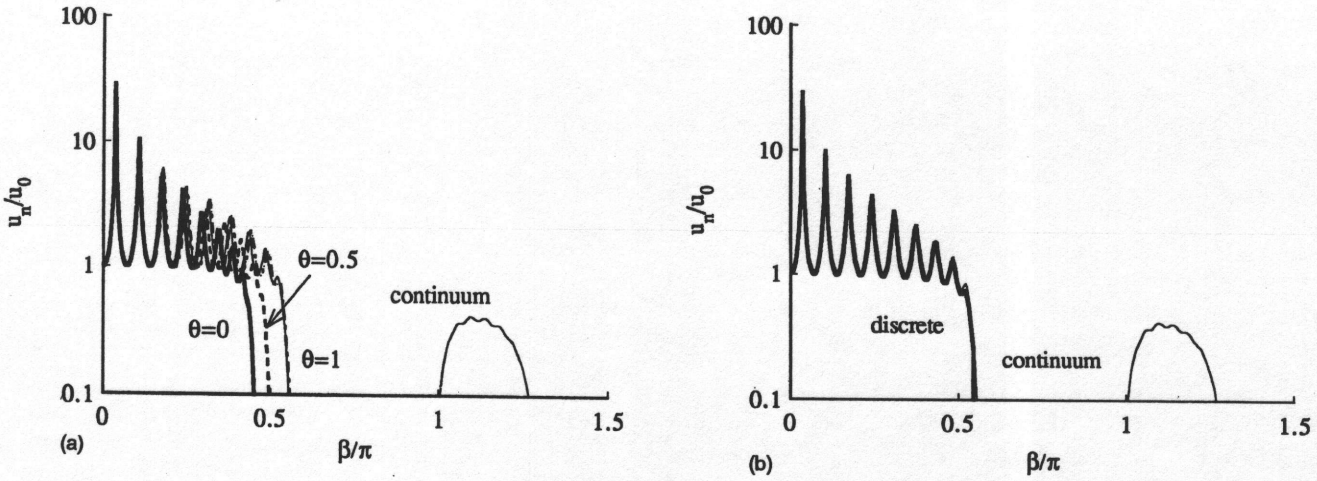

Figure 11. Frequency response function of continuum with added mass ($\alpha = 1.0$): (a) $\theta = 0, 0.5, 1$; (b) $\theta = \theta_{opt}$

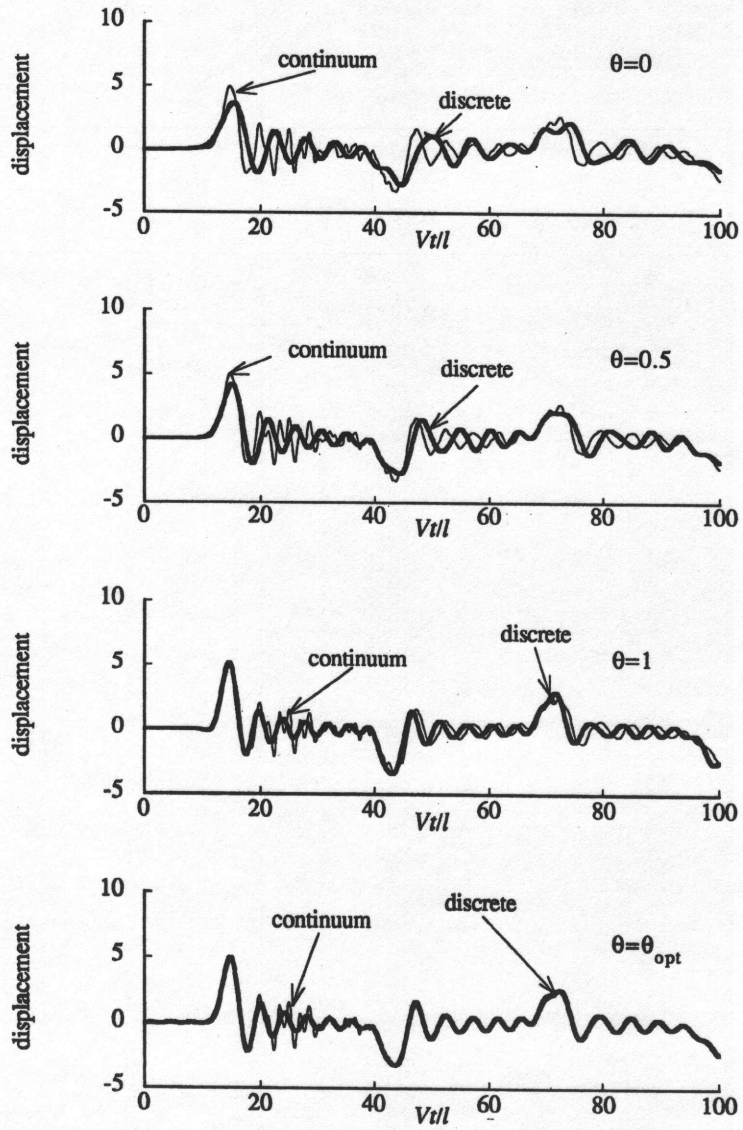

Figure 12 Impulse response function of continuum with added mass ($\alpha = 1{\cdot}0$)

This section concludes by comparing the frequency response functions and impulse response functions for different models of the periodic structure. Results are computed for displacement response at the right end of the structure due to a unit harmonic displacement prescribed at the left end, where $n = 10$, material damping ratio gets ratio $h = 0{\cdot}01$ and $\alpha = 0$. Figure 9 compares the frequency response functions of the continuum model and those of the discrete models with consistent mass ratios $\theta = 0$, $\frac{1}{2}$, 1 and θ_{opt}. The comparison shows that the discrete model with $\theta = \frac{1}{2}$ gives results which are closer to those of the continuum model than models with $\theta = 0$ or 1. This can be expected from the behaviour of the phase and group velocities, shown in Figure 5. When the optimal consistent mass ratio is used, the discrete model gives almost identical results with those of the continuum model up to the frequency $\beta = 0{\cdot}6\pi$. Figure 10 shows the corresponding impulse response functions, where frequency increment $\Delta\beta = 0{\cdot}005$ and Nyquist frequency $\beta_{max} = 163{\cdot}84$ are used for fast Fourier transform. Since the waves are not dispersive in case of the continuum model, the response shows the repeating pulses which consist of transmitting and reflecting waves. On the other hand, the discrete model shows the dispersive results where the pulses are deformed. Especially, the discrete model using consistent mass ($\theta = 1$) or lumped mass ($\theta = 0$) gives undesirable results. As a result, the consistent mass ratio should be selected as $\theta = \frac{1}{2}$ or θ_{opt} in the case of homogeneous continuum such as soil.

Figures 11 and 12 show corresponding results for the continuum with added masses ($\alpha = 1$). The stop band emerges and the waves become dispersive due to the existence of added masses even for the continuum model. In this case, the discrete model with $\theta = 1$ or θ_{opt} gives a good result compared to other discrete models. From these comparisons it is clarified that the results obtained by a discrete model using the optimal consistent mass ratio are accurate in a wider frequency range, compared to those of the usual discrete models. The pass band is also extended when using the optimal consistent mass ratio. Several general trends of the dynamic property of the periodic structure can also be observed in Figures 11 and 12. The resonance peaks are most prominent at low frequencies, particularly when the lumped masses are added. The response is small at the stop bands. When the magnitude of the lumped masses increases, the stop bands become wider and the response at the stop band frequencies become smaller.

5. CONCLUSIONS

Wave propagation in a one-dimensional periodic structure is studied using the wave solution of the continuum and the finite element solution combined with the transfer matrix method. The main results and conclusions of the study are:

1. The wave solution and the finite element solution of one-dimensional continuum can be combined with the transfer matrix method to obtain the response of the periodic structure. By careful consideration of the eigenvalues of the transfer matrix, numerical instabilities are avoided.
2. The eigenvalues of the transfer matrix are used to determine explicit expressions for the phase and group wave velocities. Furthermore, to quantify wave attenuation, a spatial attenuation rate is developed.
3. The existence of lumped masses in the periodic structure results in stop and pass bands and a dispersion of the wave velocities.
4. For frequencies in the first pass band, the continuum model can be approximated by a discrete model. The discrete model shows a numerical dispersion which depends on mass modelling. When a homogeneous continuum such as a soil is considered, an average of lumped and consistent masses shows good results while a consistent mass model is adequate when the lumped masses exist as in the case of a high-rise building.
5. By fitting the discrete results to the continuum results, an optimal mass model is proposed. The resulting consistent mass ratios yield the most accurate discrete model.

ACKNOWLEDGEMENT

The authors would like to express their appreciation to Dr. H. Katukura and Dr. S. Nakai of Ohsaki Research Institute, Shimizu Corporation, and Professor Takeru Igusa of Northwestern University for their helpful suggestions.

REFERENCES

1. L. Brillouin, *Wave Propagation in Periodic Structures*, Dover, New York, 1953.
2. D. J. Mead, 'A new method of analyzing wave propagation in periodic structures; applications to periodic Timoshenko beams and stiffened plates', *J. sound vib.* **104**, 9–27 (1986).
3. D. J. Mead, 'Free wave propagation in periodically-supported infinite beams', *J. sound vib.* **11**, 181–197 (1970).
4. Y. K. Lin and T. J. McDaniel, 'Dynamics of beam-type periodic structures', *J. eng. ind. trans. ASME*, **91**, 1133–1141 (1969).
5. Y. Yong and Y. K. Lin, 'Dynamics of complex truss-type space structures', *Proc. 30th conf. on structures, structural dynamics and materials*, 1989, pp. 1295–1304.
6. E. C. Pestel and F. A. Leckie, *Matrix Methods in Elastomechanics*, McGraw-Hill, New York, 1963.
7. N. A. Haskel, 'The dispersion of surface waves of multi-layered media', *Bull. seism. soc. Am.* **43**, 14–34 (1953).
8. G. L. Goudreau, 'Evaluation of discrete methods for the linear dynamic response of elastic and viscoelastic solids', *UC SESM Report 69-15*, University of California, Berkeley, 1970.
9. T. J. R. Hughes, *The Finite Element Method; Linear Static and Dynamic Finite Element Analysis*, Prentice-Hall, Englewood Cliffs, NJ, 1987.
10. R. J. Melosh and H. A. Smith, 'New formulation for vibration analysis', *J. eng. mech. ASCE* **115**, 543–554 (1989).